Methanethiol Adsorption on Defective MoS_2(0001) Surfaces

Christopher G. Wiegenstein[†]

Department of Chemical and Natural Gas Engineering, Texas A&M University—Kingsville, Campus Box 193, Kingsville, Texas 78363

Kirk H. Schulz*[,‡]

Department of Chemical Engineering, Michigan Technological University, 1400 Townsend Drive, Houghton, Michigan 49931

Received: March 15, 1999; In Final Form: June 15, 1999

There have been relatively few studies that have used molybdenum sulfide single crystals as model HDS catalysts. MoS_2(0001) single crystal surfaces are largely unreactive toward many organosulfur compounds but can be ion-bombarded to form chemically active surfaces with large densities of sulfur vacancies (coordinately unsaturated Mo sites). XPS and AES measurements confirm that sulfur is preferentially removed during ion-bombardment and that significant changes occur in the distribution of Mo oxidation states at the surface as a function of ion-bombardment time. Methanethiol adsorption studies were performed using TPD on ion-bombarded MoS_2(0001) single-crystal surfaces. Methanethiol, methane, ethane, and ethylene were observed as decomposition products, which are thought to arise from methanethiolate and thioformaldehyde surface intermediates. Additionally, product selectivity varied as a function of *cus* Mo surface site densities.

Introduction

Hydrodesulfurization (HDS) is an important reaction in the processing of crude oil into usable products. HDS is characterized by the removal of a sulfur atom from an organosulfur molecule. The main reason for sulfur removal is that sulfur is a catalyst poison, especially for the platinum group catalysts used in the hydrocracking process. There is renewed interest in HDS within the automotive industry that is calling for a reduction of the amount of sulfur contained in gasoline from 300 to 30 ppm.[1,2] The reason behind the reduction of gasoline sulfur is due to sulfur poisoning of automobile catalytic converters. Additionally, the Environmental Protection Agency has put a restriction on the amount of SO_2 that automobiles can emit.[3]

Industrially, the catalyst used for HDS is molybdenum disulfide supported on alumina promoted with cobalt.[4] Molybdenum disulfide (MoS_2) is an important catalyst used in a variety of chemical processing applications, including hydrogenation reactions,[5,6] Fischer−Tropsch synthesis of alcohols,[7] and hydrodesulfurization (HDS) reactions.[4,8−10] Much of the work on understanding the catalytic properties of MoS_2 has focused on HDS reactions, particularly of aromatic organosulfur compounds such as thiophene. The study of HDS reactions revolves around three principle elements. Each of the three must be studied in order to gain a complete understanding of the catalytic role of MoS_2 in HDS reactions. The first element is the physical and chemical properties of the catalyst material, the second element is the nature of the organosulfur compound undergoing desulfurization, and the third element is the interaction of hydrogen with the catalyst surface. Even though there has been a significant amount of work done on HDS catalysts, there is still no complete understanding of the roles each of these elements play in HDS reactions. This is primarily because few ideal model systems exist to study the effect that each element has on HDS activity. One solution to this problem is to use single crystals as model catalyst materials. Indeed, single crystals have been successfully used on several occasions as model catalysts.[13−15]

The properties of MoS_2-based catalysts and reactions involving various organosulfur molecules have been the subject of many experimental studies.[4,8−12] However, only a few studies have been conducted on the MoS_2(0001) surface, and none have examined the HDS of methanethiol. The reason for choosing methanethiol as the reactant is the ease with which it carries out HDS reactions, making it a good probe molecule to examine changes in surface reactivity. Additionally, it will be the easiest for which to determine the surface intermediates because of its relatively simple molecular structure.

The MoS_2(0001) surface has been shown to be catalytically inactive toward thiophene (C_4H_4S), as determined by a lack of any detectable reaction product during TPD experiments.[16,17] Additionally, AES spectra showed no increase in surface carbon, which further substantiates the absence of thiophene decomposition.[16,17] However, this surface did react with ethanethiol,[17] which suggests that some surface defects (i.e., sulfur vacancies) are present on a freshly cleaved basal surface. The role of surface defects in HDS reactions have not been reported in the literature. Roxlo et al. suggest that an ion-bombarded surface might be active toward thiophene HDS, but no results were reported to support this statement.[18]

Methanethiol adsorption has been studied on a wide variety of metal single-crystal surfaces. The intermediates proposed and reaction products observed for methanethiol on several of these surfaces are summarized in Table 1. On all surfaces except the Au(111) surface, the S−H bond was cleaved below 200 K. The resulting methanethiolate can then react in three distinct

* To whom correspondence should be addressed.
[†] Phone: (361) 593-2094. Fax: (512) 593-2106. E-mail: kfcgw00@tamuk.edu.
[‡] Phone: (906) 487-3204. Fax: (906) 487-3213. E-mail: khschulz@mtu.edu.

10.1021/jp990896y CCC: $18.00
Published on Web 08/03/1999

TABLE 1: Methanethiol Surface Intermediates and Reaction Products for Several Metal Single Crystals

surface	intermediates	products	ref
Ni(100)	CH_3S-	C_1	19−21
Ni(110)	CH_3S-	C_1	22
Ni(111)	NA[a]	C_1, C_2	23
Fe(100)	CH_3S-, CH_3-	C_1	24
Cu(111)	CH_3S-	NA[b]	20, 25
Cu(100)	CH_3S-	C_1	26
W(001)	CH_3S-, CH_3S[c]	C_1	27
W(211)	CH_3S-, CH_2S-	C_1, C_2	28
Pt(111)	CH_3S-, CH_2S-, $CHS-$	C_1	29, 30
Au(111)	CH_3SH	C_1	31
Mo(110)	CH_3S-	C_1	32

[a] Spectroscopic data not available. [b] Product data not available. [c] Two thiolate intermediates reported.

pathways: recombination with hydrogen to reform methanethiol, hydrogenation coupled with C−S bond cleavage to form methane, and (or) complete dehydrogenation to form surface carbon. Other organosulfur intermediates were also observed. On the W(211)[28] and Pt(111)[29,30] surfaces, a thioformaldehyde ($H_2C{=}S$) species was reported. Additionally, two different groups observed products formed from C_1 coupling reactions to form ethane, although surface intermediates were not identified.

The present study looks at the adsorption of methanethiol on air-cleaved and ion-bombarded MoS_2(0001) surfaces to elucidate the role of surface defects on HDS reaction pathways on MoS_2 based catalyst surfaces.

Experimental Section

Surface Structure. The surface of an MoS_2 single crystal is a large sulfur terminated plane termed the "basal surface". Molybdenum disulfide is a layered material that consists of three "planes" of atoms (sulfur−molybdenum−sulfur) weakly bound together by van der Waals forces. These repeat units consist of two layers of S(−II) sulfur anions that bond to a layer of Mo(+VI) cations. Two stable edge planes have also been identified for MoS_2, which includes the $(\bar{1}010)$ and $(10\bar{1}0)$ surfaces.[33] Each of the three different planes has a different bonding configuration for sulfur. The (0001) basal sulfur atoms form three bonds, the $(10\bar{1}0)$ surface sulfur atoms form one bond, and the $(\bar{1}010)$ surface has doubly bridged sulfur species.[34,35] However, only the MoS_2 basal planes grow large enough to perform routine surface science studies and, thus, are used as a model catalytic system for our study.

Experimental Equipment. All experiments were performed in an ion-pumped, stainless steel, single chamber ultrahigh vacuum (UHV) system. Vacuum was achieved using a 240 L/s Thermionics TTS-240N ion pump with a Varian SD300 mechanical roughing pump used to differentially pump the rotary platform of the sample manipulator. The normal operating pressure of the system during experimentation was $\sim 1 \times 10^{-9}$ Torr. The chamber is equipped with an Omicron Vakuumphysik Spectaleed L-A-2000 unit, capable of both low-energy-electron diffraction (LEED) and Auger electron spectroscopy (AES). For AES measurements, the unit is operated as a retarded field analyzer with an incident electron beam energy of 1.5 kV and a resolution of $\Delta E/E = 0.45\%$. The analyzer is interfaced with a 486-based personal computer operating the Omicron Auger Control Software (ACS, Version 4.0). LEED experiments were performed using the unit as a reverse-view four grid LEED optics system.

Sample manipulation was performed using a Thermionics EC-1275-XYZ manipulator equipped with a RNN-150/FA differentially pumped rotary seal (capable of 360° of sample rotation), allowing sample alignment with each port in the vacuum chamber. A sample was mounted on a 0.5 mm thick tantalum sheet and mechanically held in place using stainless steel screws. The sample temperature was monitored using a type K thermocouple held in contact with the back of the tantalum foil via spot welding. This assembly was then mounted on copper blocks fastened to the manipulator. The sample was resistively heated by passing current through the tantalum sheet, while the sample cooling was by conduction through the copper blocks in thermal contact with liquid nitrogen. The sample mounting arrangement has been described in more detail elsewhere.[36]

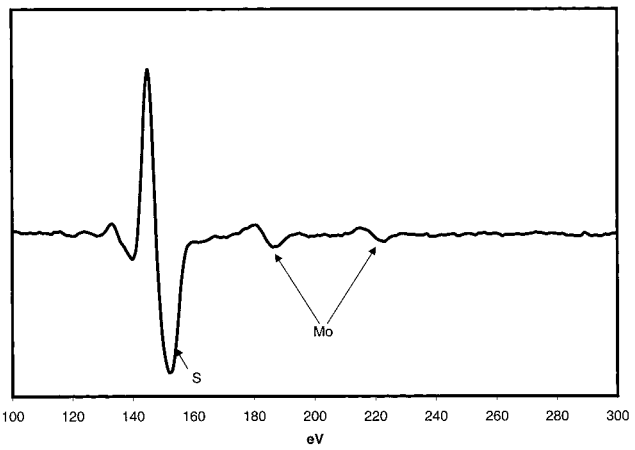

Figure 1. Typical AES spectrum for MoS_2(0001).

Temperature-programmed desorption (TPD) experiments were performed using a Leybold Inficon Transpector H200M quadropole mass spectrometer. The mass spectrometer sensing unit was fitted with a quartz nose cone containing a 1 mm hole, which minimizes background desorption signals from the manipulator and sample support hardware. The program used to collect the TPD data is described elsewhere.[37]

Sample gases were introduced into the vacuum system through a vacuum-pumped dosing line connected to the UHV system. Sample dosing was accomplished by back-filling the vacuum chamber using a Varian variable leak valve. All reactant exposures were measured in Langmuirs ($1\ L = 10^{-6}$ Torr s).

MoS_2 samples were obtained from Wards Earth Science. Argon (99.9999%, Nova Gas Technologies) and methanethiol (99.5+%, Aldrich) were used in experimental studies as received.

Results

Surface Preparation. *MoS_2(0001) Surface.* The MoS_2 samples used were air-cleaved prior to mounting within the UHV system. A freshly cleaved surface was prepared by peeling away the top few layers using a piece of cellophane tape. This procedure yielded sections of the sample that were clearly single crystalline. Once in the UHV system, the MoS_2 sample produced a hazy (1×1) hexagonal LEED pattern that verifies a single-crystal structure. After annealing the sample to ~950 K for 10 min, the pattern sharpened. The sample size was approximately 15 mm × 15 mm × 1 mm, and uniform LEED patterns were not observed across the entire sample. The single crystal regions on the sample were approximately 3 mm square and were used exclusively for the TPD experiments described here. AES widescans showed no peaks other than molybdenum (186, 221 eV) and sulfur (152 eV), as shown in Figure 1. The uncorrected AES S(LMM)-to-Mo(MNN) ratio for a freshly cleaved sample was ~14, which is similar to the S/Mo ratio reported in other

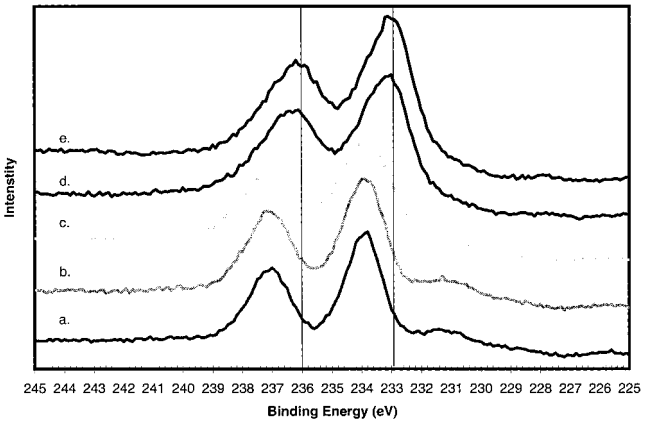

Figure 2. XPS spectra of the Mo 3d peaks as a function of ion-bombardment time.

MoS_2 (0001) studies.[16,20] No significant change in the S/Mo ratio was observed upon annealing the surface at 1000 K. Additionally, no detectable electron beam damage to the MoS_2 sample was observed following AES or LEED experiments.

Defective Surfaces. Defective MoS_2 surfaces were prepared by ion-bombarding a cleaved MoS_2(0001) sample for a given time prior to TPD experiments. Ion-bombardment was carried out by back-filling the vacuum chamber with $\sim 2.0 \times 10^{-5}$ Torr of argon. AES wide scans only show peaks attributed to Mo and S for each sample. The uncorrected AES S(LMM)-to-Mo(MNN) ratio decreased from 14 ± 2.2 to 7.6 ± 1.2 with 30 s of ion bombardment and to 5.9 ± 0.1 after 60 s of ion bombardment. The S-to-Mo ratio did not change upon annealing any of the ion-bombarded samples to 1000 K.

To understand changes in oxidation state during ion-bombardment, XPS measurements were performed on the MoS_2-(0001) surface as a function of ion-bombardment time. Figure 2 shows changes that occurred in Mo 3d peaks as a function of sample treatment. The spectrum for a freshly air cleaved surface, Figure 2a, shows Mo 3d peaks consistent with Mo(+IV). No significant change in peak positions or intensity was observed following annealing of the sample in (a) to 573 K, as illustrated in Figure 2b. This illustrates that annealing of the freshly cleaved surface did not result in any significant change in Mo oxidation state. Following ion bombardment for 2 min, the Mo 3d peaks broaden slightly, which suggests that additional Mo oxidation states at higher binding energy are present at the surface. This is illustrated in Figure 2c. Following further ion-bombardment (10 min) a significant change in the ratio of Mo oxidation states at the surface was observed. This is illustrated most strongly by a shift in the Mo 3d peak position to higher binding energy, which corresponds to a higher concentration of additional Mo oxidation states at the surface. Further ion bombardment (50 min) had no significant effects on the peak position, as illustrated in Figure 2e. Because of the relatively complex surface structure at longer ion-bombardment times, all TPD experiments were performed on surfaces formed after short ion-bombardment times, which would most closely correspond to XPS spectra a−c.

Methanethiol Adsorption on MoS_2(0001) Freshly Cleaved. For all TPD experiments, the sample was initially cooled to 100 K, and then methanethiol was dosed on the surface by back-filling the chamber, rotated in front of the mass spectrometer, and heated to 1000 K. A heating rate of 2 K/s was used for all TPD experiments. The ceramic nature of MoS_2 precluded using higher heating rates. Selected desorption traces, representative of the majority of the TPD experiments performed, are given

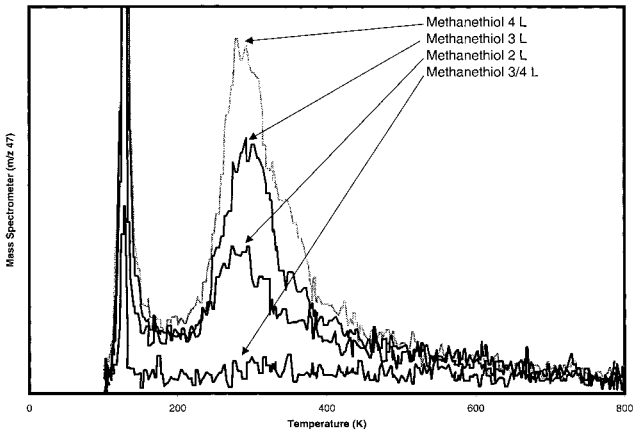

Figure 3. Temperature-programmed desorption spectra as a function of increasing coverage for methanethiol from MoS_2(0001).

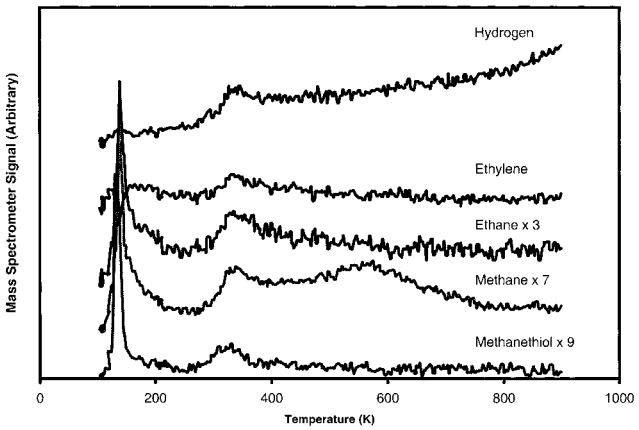

Figure 4. Temperature-programmed desorption spectra for desorption products for a 3 L dose of methanethiol from MoS_2(0001). Spectra have been multiplied by arbitrary factors to scale them to the same relative size.

in all of the TPD figures. All doses reported in this paper have been corrected for mass spectrometer and ion gauge sensitivity.[39,40]

Methanethiol TPD experiments were conducted on cleaved MoS_2(0001) samples. Methanethiol desorption as a function of increasing coverage is shown in Figure 3. Peaks were observed at ~125 K and ~300 K. The 300 K grows in at higher coverages and eventually saturates. The 125 K peak continues to grow at increasing coverages, which suggests this peak is due to multilayer formation. Assuming a first-order desorption process and a preexponential factor of 10^{13} s^{-1},[41] the 125 and 300 K peaks have activation energies of 7.6 and 18.7 kcal/mol, respectively.

Reaction products from a 3 L TPD of methanethiol are shown in Figure 4. Hydrogen, methane, ethylene, and ethane were detected as reaction products. All products except methane, ethylene, and hydrogen desorbed in the same temperature range as methanethiol. Ethylene, methane, and hydrogen were also observed in a peak at ~300 K peak. A peak was also observed at 575 K for methane that corresponds to an activation energy of 36.6 kcal/mol. This high-temperature CH_4 peak may be due to "burn off" of residual surface carbon with surface hydrogen. Mass-to-charge ratios sampled during all TPD experiments include 2, 15, 16, 26, 27, 28, 29, 30, 32, 34, 45, 47, 48.

Methanethiol Adsorption on Ion-Bombarded MoS_2. The TPD experiments on ion-bombarded MoS_2 surfaces were conducted in the same manner as on the cleaved MoS_2(0001) surface. Ion bombardment was completed by back-filling the

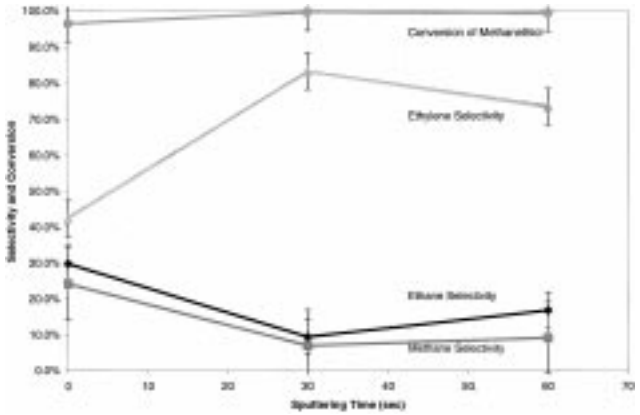

Figure 5. Methane, ethane, and ethylene selectivity and methanethiol conversion plotted as a function of ion bombardment on $MoS_2(0001)$.

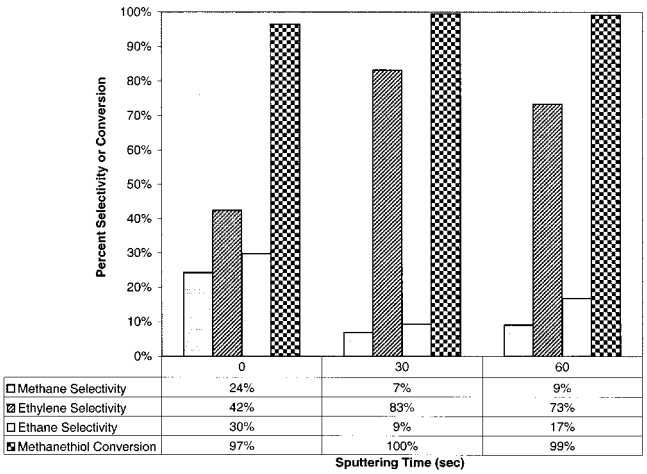

	0	30	60
Methane Selectivity	24%	7%	9%
Ethylene Selectivity	42%	83%	73%
Ethane Selectivity	30%	9%	17%
Methanethiol Conversion	97%	100%	99%

Figure 6. Selectivity and total conversion for the products of a 3 L methanethiol TPD as a function of ion bombardment.

chamber to $\sim 5.0 \times 10^{-5}$ Torr with argon. A beam voltage of 1.5 kV and an emission current of 25 mA were used for the ion gun. Ion bombardment was carried out for 30 s increments, and times are reported as the sum of all previous ion-bombardment treatments. After each ion-bombardment cycle the sample was exposed to methanethiol.

Increased ion-bombardment time did not significantly change the methanethiol decomposition products. The peaks remained at the same relative temperature, and no new products were observed. However, the selectivity of the reaction products did change as a function of ion-bombardment time. Figure 5 shows the effect of ion-bombardment on the selectivity of methane, ethane, ethylene, and methanethiol. Following a 30 s ion-bombardment treatment, methane and ethane selectivity decreased, while ethylene selectivity increased. Further ion-bombardment resulted in no significant changes in selectivity. Figure 6 summarizes the changes that occurred in product selectivity and conversion of a 3 L methanethiol dose as a function of ion-bombardment time.

AES measurements were taken prior to and immediately following TPD runs. AES scans indicated that after 30 s of ion bombardment the AES S/Mo ratio decreased from 14 ± 2.2 to 7.6 ± 1.2. After exposing the surface to 3 and 10 L doses of methanethiol, the AES S/Mo ratio had increased to 8.3 ± 0.5. An additional 60 s of ion-bombardment decreased the AES S/Mo ratio to 5.9 ± 0.1. After the surface was exposed to 3 and 10 L doses of methanethiol, the AES S/Mo ratio increased to 6.2 ± 0.1. The AES results suggest that ion-bombardment is preferentially removing surface sulfur atoms and that sulfur is left behind on the surface following methanethiol TPD experiments.

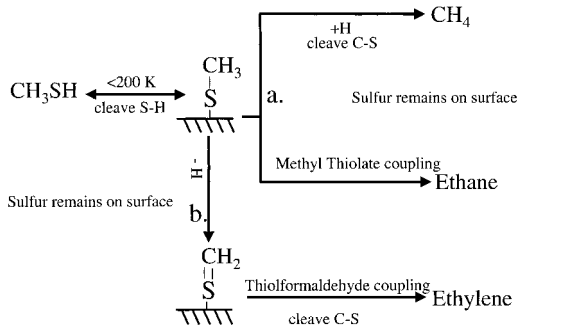

Figure 7. Proposed reaction pathways for methanethiol hydrodesulfurization on MoS_2 defective surfaces.

Discussion

Reaction Pathway. The proposed reaction pathway of methanethiol on the $MoS_2(0001)$ surface is shown in Figure 7. Although we have no firm spectroscopic evidence for the intermediate species, the observed product distribution and observation of similar product molecules from methanethiol studies in the literature are sufficient to propose a plausible mechanism. Methanethiol adsorbs through the sulfur atom to a sulfur vacancy, at which time it cleaves the S−H bond, forming a methanethiolate surface intermediate. The methanethiolate binds to the surface through the sulfur directly to a Mo atom. It is unlikely that the methanethiolate will bind to a sulfur atom, because it will only form a weak bond that will break at very low temperatures. This is primarily due to the fact that sulfur on the surface has filled p electron orbitals and, thus, has no open bonding sites for single electrons.

The methanethiolate can then react to re-form methanethiol, hydrogenate to form methane, couple with another methanethiolate to form ethane, or dehydrogenate forming a thioformaldehyde surface intermediate. The methanethiolate species can recombine with hydrogen, forming methanethiol, as observed on most of the metal single-crystal surfaces. Methanethiolate surface intermediates can hydrogenate to form methane, which was also observed on metal single-crystal surfaces. Indeed, on a Ni(111) surface, adsorbed surface deuterium was shown to incorporate into adsorbed intermediates to form deuterated methane.[23] In an alternate pathway, methanethiolate couples with another methanethiolate to form ethane. This coupling of methanethiolate surface species has been reported on Ni(111)[23] and W(211)[28] surfaces. The final surface reaction is thought to be dehydrogenolysis of the methanethiolate to form a thioformaldehyde intermediate, which has been reported on W(211)[28] and Pt(111)[29,30] surfaces. In methanol reactivity studies on many metal surfaces an analogous reaction has been observed where methoxy (CH_3O-) species react to form formaldehyde.[42−49]

We propose the thioformaldehyde species can recombine with another thioformaldehyde or a methanethiolate to form ethylene. Although there is no direct spectroscopic evidence for this surface reaction, the other pathway for the formation of ethylene is the dehydrogenation of ethane, which seems unlikely on this surface. Further information about the surface reactivity of thioformaldehyde species can only be obtained by conducting vibrational spectroscopic studies of the surface intermediates.

Selectivity Changes as a Function of Ion Bombardment. Ion bombardment of the surface for short periods of time increases the activity toward methanethiol adsorption. This is

thought to occur due to an increase in the number of *cus* Mo sites. This is consistent with both the XPS and AES results, which showed decreasing sulfur signal as a function of ion-bombardment time and the corresponding shifts in oxidation state. Ion bombardment increased the selectivity of the dehydrogenation pathway (pathway b in Figure 7) and decreased the selectivity of the hydrogenation pathway (pathway a in Figure 7). The enhancement of the dehydrogenation pathway is thought to occur due to an increase in *cus* Mo sites following ion bombardment. A similar trend was observed by Aoshima and Wise, who reported an increase in the dehydrogenation and decomposition of butanethiol over MoS_2(0001) surfaces as surface sulfur vacancies increased.[50] Additionally, this trend is consistent with methanethiol studies on the Mo(110) surface,[32] which show complete dehydrogenation of adsorbates to surface carbon, sulfur, and hydrogen.

In these experiments, insight into the reaction pathways was also obtained by performing a series of TPD experiments and allowing the surface sulfur to accumulate. Because sulfur was left behind at the end of the first TPD run, a second TPD experiment of an identical coverage was conducted. A significant change in the total amount of hydrocarbon products desorbing from the surface was observed between TPD experiments. The increase in total hydrocarbon product yield noted after ion bombardment shows that ion bombardment is removing surface sulfurs to form additional *cus* Mo sites active for HDS reactions. However, the decrease in hydrocarbon products observed following the second TPD run (on the surface where sulfur was allowed to accumulate) shows the *cus* Mo sites become blocked with adsorbed sulfur atoms, thus decreasing the "active" surface sites for chemical adsorption.

Finally, the sulfur defect sites increase with ion-bombardment to a point where ion-bombardment starts to transform the surface to one with mixed oxidation states, which seems to have a more metallic nature compared with short ion-bombardment times. The formation of *cus* Mo sites favors an increase on HDS activity, but it also increases the dehydrogenation of the methanethiolate species to thioformaldehyde, which in turn results in an increase in the amount of ethylene formed. The increase in HDS activity is due to the increase in sites that can strongly bind with the sulfur in the methanethiolate surface intermediate and subsequently break the C−S bond. The increase in ethylene formation is most likely because the surface has a high affinity for hydrogen,[51] causing the dehydrogenation reaction of the methanethiolate species to be favored.

Relevance to HDS Catalysis. Although methanethiol is not the standard industrial HDS molecule, it makes for a good probe molecule. Our study confirms that *cus* Mo atoms are the key catalytic sites. Our experiments also show that the concentration of these *cus* Mo sites has a direct effect on the hydrogenation and dehydrogenation pathways. The surface pathways proposed for methanethiol will hopefully help in determining the reaction pathways for more complex organosulfur molecules, particularly pathways that involve thiophene or thiolate-like thiophene intermediates.[52]

Conclusions

Our experiments represent the first study to examine methanethiol adsorption on defective MoS_2(0001) surfaces. They also represent the first study to directly examine the role of *cus* Mo sites on HDS activity. We have shown that we can prepare a reactive surface by using ion-bombardment and that reactivity can be varied in a controlled fashion. Additionally, the *cus* Mo sites are the key to HDS activity, and the concentration of the *cus* Mo sites can affect the reaction pathways. Our studies also suggest that the two key surface intermediates for methanethiol HDS are methanethiolate and thioformaldehyde. The methanethiolate species is hypothesized to react in three distinct pathways: hydrogenation reaction to form methane, a coupling reaction to form ethane, and a dehydrogenation reaction to form the thioformaldehyde species. The thioformaldehyde species can react further to form the methanethiolate intermediate or couple to form ethylene.

Acknowledgment. The authors gratefully acknowledge the NSF for funding this project under CTS-9523936 and George Graham of the Ford Motor Co. for his help in taking the XPS data.

References and Notes

(1) *The Detroit News* **1998**, Wed. May 13.
(2) AAMA Press Release, March 19, 1998.
(3) EPA Staff Paper on Gasoline Sulfur Issues, EPA420-R-98-005, May 1, 1998.
(4) Startesev, A. N. *Catal. Rev.—Sci. Eng*. **1995**, *37*, 353.
(5) Jalowiecki, L.; Grimblot, J.; Bonnelle, J. P. *J. Catal*. **1990**, *126*, 101.
(6) Wambeke, A.; Jalowiecki, L.; Kasztelan, S.; Grimblot, J.; Bonnelle, J. P. *J. Catal*. **1988**, *109*, 320.
(7) Dianis, W. P. *Appl. Catal*. **1987**, *30*, 99.
(8) Grange, P. *Catal. Rev.—Sci. Eng*. **1980**, *21*, 135.
(9) Delmon, B. In *Chemistry and Uses of Molybdenum*; Barry, H. F., Mitchell, P. C. H., Eds.; Proceedings Climax 3rd International Conference; Climax Molybdenum Company: Ann Arbor, MI, 1979; pp 73−84.
(10) Prins, R.; DeBeer, V. H. J.; Somorjai, G. A. *Catal. Rev.—Sci. Eng*. **1989**, *31*, 1.
(11) Ratnasamy, P.; Sivasanker, S. *Catal. Rev.—Sci. Eng*. **1980**, *22*, 401.
(12) Chianelli, R. R.; Daage, M.; LeDoux, M. J. *Adv. Catal*. **1994**, *40*, 177.
(13) Goodman, D. W. *Acc. Chem Res*. **1984**, *17*, 194.
(14) Boudart, M. *Chemtech* **1986**, 688.
(15) Gerhard, E.; Freund, H. J. *Physics Today* **1999**, January, 32.
(16) Salmeron, M.; Somorjai, G. A.; Wold, A.; Chianelli, R.; Liang, K. S. *Chem. Phys. Lett*. **1982**, *90*, 105.
(17) Peterson, S. L.; Schulz, K. H. *Langmuir* **1996**, *12*, 941.
(18) Roxlo, B.; Deckman, H. W.; Gland, J.; Cameron, S. D.; Chianelli, R. *Science* **1987**, *56*, 1629.
(19) Castro, M. E.; Ahkter, S.; Golchet, A.; White, J. M.; Sahin, T. *Langmuir* **1991**, *7*, 126.
(20) Parker, B.; Gellman, A. J. *Surf. Sci*. **1993**, *292*, 223.
(21) Bao, S.; McConville, C. F.; Woodruff, D. P. *Surf. Sci*. **1987**, *197*, 133.
(22) Huntley, D. R. *J. Phys. Chem*. **1989**, *93*, 6156.
(23) Castro, M. E.; White, J. M. *Surf. Sci*. **1991**, *257*, 22.
(24) Albert, M. R.; Lu, J. P.; Bernasek, S. L.; Cameron, S. D.; Gland, J. L. *Surf. Sci*. **1988**, *206*, 348.
(25) Seymour, D. L.; Bao, S.; McConville, C. F.; Crapper, M. D.; Woodruff, D. P.; Jones, R. G. *Surf. Sci*. **1987**, *189/190*, 529.
(26) Sexton, B. A.; Nyberd, G. L. *Surf. Sci*. **1986**, *165*, 251.
(27) Mullins, D. R.; Lyman, P. F. *J. Phys. Chem*. **1993**, *97*, 9226.
(28) Benziger, J. B.; Preston, R. E. *J. Phys. Chem*. **1985**, *89*, 9, 5002.
(29) Rufael, T. S.; Koestner, R. J.; Kollin, E. B.; Salmeron, M.; Gland, J. L. *Surf. Sci*. **1993**, *297*, 272.
(30) Koestner, R. J.; Stöhr, J.; Gland, J. L.; Kollin, E. B.; Sette, F. *Chem. Phys. Lett*. **1985**, *120*, 285.
(31) Nuzzo, R. G.; Zegarski, B. R.; Dubois, L. H. *J. Am. Chem. Soc*. **1987**, *109*, 773.
(32) Wiegand, B. C.; Uvdal, P.; Friend, C. M. *Surf. Sci*. **1992**, *279*, 105.
(33) Kasztelan, S.; Toulhoat, H.; Grimblot, J.; Bonnelle, J. P. *Appl. Catal*. **1984**, *13*, 127.
(34) Wambeke, A.; Jalowiecki, L.; Kasztelan, S.; Grimblot, J.; Bonnelle, J. P. *J. Catal*. **1988**, *109*, 320.
(35) Kasztelan, S. *Langmuir* **1990**, *6*, 590.
(36) Peterson, S. L.; Schulz, K. H.; Schulz, C. A., Jr.; Vohs, J. M. *Rev. Sci. Instrum*. **1995**, *66*, 3048.
(37) Wiegenstein, C. G.; Schulz, K. H.; Scott, J. *Rev. Sci. Instrum*. **1998**, *69*, 3707.
(38) Feng, H. C.; Chen, J. M. *J. Phys. C: Solid State Phys*. **1974**, *7*, L75.
(39) Ion gauge sensitivities of 0.75, 3.18, and 0.78 were used for methane, ethane, and ethylene, respectively. These ion gauge sensitivities were calculated using a correlation attributed to S. George for hydrocarbons reported in ref 40.

(40) Brainard, R. L.; Madix, R. J. *J. Am. Chem. Soc.* **1989**, *11*, 3826.
(41) Redhead, P. A. *Vacuum* **1962**, *12*, 203.
(42) Lu, J. P.; Albert, M.; Bernasek, S. L.; Dwyer, D. S. *Surf. Sci.* **1989**, *218*, 1.
(43) Akhter, S.; Cheng, W. H.; Lui, K.; Kung, H. H. *J. Catal*. **1984**, *85*, 437.
(44) Hirschwald, W.; Hofmann, D. *Surf. Sci.* **1984**, *140*, 415.
(45) Vohs, J. M.; Barteau, M. A. *Surf. Sci.* **1986**, *176*, 91.
(46) Vohs, J. M.; Barteau, M. A. *Surf. Sci.* **1988**, *197*, 109.
(47) Wachs, I. E.; Madix, R. J. *J. Catal*. **1978**, *53*, 208.
(48) Bowker, M.; Madix, R. J. *Surf. Sci*. **1980**, *95*, 190.
(49) Cox, D. F.; Schulz, K. H. *J. Vac. Sci. Technol. A.* **1990**, *8*, 2599.
(50) Aoshima, A.; Wise, H. *J. Catal.* **1974**, *34*, 145.
(51) Wiegenstein, C. G.; Schulz, K. H. *Surf. Sci.* **1998**, *396*, 284.
(52) Lipch, J. M. J. G.; Schuit, G. C. A. *J. Catal.* **1969**, *15*, 179.